## Supporting Information

**Bis(pyridyl)-disulfonamides: Structural comparison with their carboxamidic analogues and effect of molecular geometry and supramolecular assembling on their photophysical properties**

*Moyna Das[a], Datta Markad[b], Suvendu Maity[c], Prasanta Ghosh[c] and Madhushree Sarkar*[a]*

[a] *Department of Chemistry, Birla Institute of Technology and Science, Pilani, Pilani Campus, Rajasthan-333031, India. Tel: +91-1596-255679; E-mail: msarkar@pilani.bits-pilani.ac.in*
[b]*Department of Chemistry, University of Liverpool, Liverpool, UK-L69 3BX*

[c] *Department of Chemistry, Narendrapur Ramkrishna Mission, Kolkata, West Bengal-700103, India. E-mail: ghosh@pghosh.in*

### Index

### Experimental

### General

$^1$H and $^{13}$C NMR spectra were recorded on a Bruker 400 MHZ spectrometer. FTIR spectra were obtained from Shimadzu IRAffinity-1S system. Powder X-Ray Diffraction (XRD) data was collected using a Rigaku miniflex II, λ =1.54 Å, Cu Kα. UV-Visible and fluorescence spectra were recorded on Jasco V-650 spectrophotometer and Fluorimax-4 0426C0809 respectively. UV-Visible absorption spectra of **L1-L3** and **L1'-L3'** were recorded by dissolving the compounds in methanol for the solution-state spectral analysis, while for the solid-state spectral analysis, the compounds were mixed with BaSO$_4$.

Gaussian-09 programme package was used for optimization of **L3** (B3LYP levels of theory with basis set 6-311++g(2d,p)).

**General procedure for the synthesis of bis(pyridyl)-disulfonamide ligands**

Compounds **L1**, **L2** and **L3** were synthesised usual condensation reaction where aminopyridine was added to disulfonyl dichloride solution in 1,4-dioxane in 1:2 molar ratio and refluxed for 6 hours. The resulting solid residue was washed with cold water and recrystallised from ethanol.

**Synthesis of *N¹,N³*-di(pyridin-2-yl)benzene-1,3-disulfonamide (L1)**

2-Aminopyridine (1.88 g, 20 mmol) was added to benzene-1,3-disulfonyl dichloride (2.75 g, 10 mmol) solution in 1,4-dioxane (50 mL) and refluxed for 6 hours. The white solid
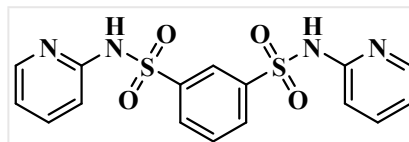


residue was washed with cold water and recrystallised from ethanol. Yield: 49%; Melting point: (242-244) °C; IR (cm⁻¹): 1670(w), 1624(m), 1531(s), 1462(m), 1381(m), 1357(m), 1130(vs), 956(m),813(s), 682(s), 578(m), 551(m) (Figure S1); $^1$H NMR (400 MHz, DMSO-$d_6$) δ ppm: 12.87 (2H, s, Amide NH), 8.30 (1H, s, ArH), 8.02 (2H, dd, $J$ = 7.8, 1.8 Hz, ArH), 7.95 – 7.90 (2H, m, ArH), 7.80 – 7.65 (3H, m, ArH), 7.16 (2H, d, $J$ = 8.8 Hz, ArH), 6.84 (2H, t, $J$ = 6.5 Hz, ArH) (Figure S2). $^{13}$C NMR (100 MHz, DMSO-$d_6$) δ ppm: 154.23, 143.81, 142.19, 130.46, 129.84, 124.66, 124.01, 115.01 (Figure S3).

**Synthesis of *N¹,N³*-di(pyridin-3-yl)benzene-1,3-disulfonamide (L2)**

3-Aminopyridine (1.88 g, 20 mmol) was added to benzene-1,3-disulfonyl dichloride (2.75 g, 10 mmol) solution in 1,4-dioxane (50 mL) and refluxed for 6 hours.
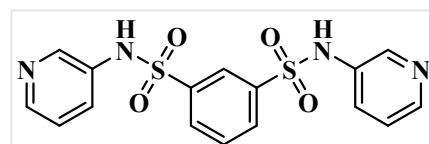


The white solid residue was washed with cold water and recrystallised from ethanol. Yield: 51%; Melting point: 239-240 °C; IR (cm⁻¹): 1585(m), 1419(m), 1357(m), 1315(m), 1265(m), 1176(m), 1157(vs), 1111(m), 933(vs), 790(s), 682(s), 578(m), 543(vs) (Figure S4); $^1$H NMR (400 MHz, DMSO-$d_6$) δ ppm: 10.82 (2H, s, Amide NH), 8.30 (2H, d, $J$ = 4.6 Hz, ArH), 8.26 – 8.20 (2H, m, ArH), 8.14 (1H, t, $J$ = 1.9 Hz, ArH), 7.97 (2H, dd, $J$ = 7.8, 1.9 Hz, ArH), 7.77 (1H, t, $J$ = 7.9 Hz, ArH), 7.41 (2H, dt, $J$ = 8.5, 1.9 Hz, ArH), 7.28 (2H, dd, $J$ = 8.3, 4.7 Hz, ArH) (Figure S5); $^{13}$C NMR (100 MHz, DMSO-$d_6$) δ ppm:146.23, 142.58, 140.58, 134.14, 131.75, 131.52, 128.60, 125.29, 124.59 (Figure S6).

**Synthesis of *N¹,N³*-di(pyridin-4-yl)benzene-1,3-disulfonamide (L3)**

4-Aminopyridine (1.88 g, 20 mmol) was added to benzene-1,3-disulfonyl dichloride (2.75 g, 10 mmol)
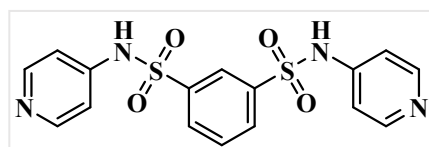
solution in 1,4-dioxane (50 mL) and refluxed for 6 hours. The white solid residue was washed with cold water and recrystallised from ethanol. Yield: 54%; Melting point: 152-155 °C; IR (cm$^{-1}$): 1635(m), 1489(vs), 1346(s), 1257(m), 1157(m), 1091(vs), 999(w), 802(vs), 783(vs), 759(s), 686(m), 586(m), 551(m) (Figure S7); $^1$H NMR (400 MHz, DMSO-$d_6$) δ ppm: 12.79 (2H, s, Amide NH), 8.15 (1H, t, $J$ = 1.8 Hz, ArH), 8.05 – 7.98 (4H, m, ArH), 7.93 (2H, dd, $J$ = 7.8, 1.8 Hz, ArH), 7.63 (1H, t, $J$ = 7.8 Hz, ArH), 6.96 – 6.90 (4H, m, ArH).(Figure S8); $^{13}$C NMR (100 MHz, DMSO-$d_6$) δ ppm: 144.73, 139.95, 130.09, 129.01, 123.82, 115.19 (Figure S9); HRMS: m/z calcd for $C_{16}H_{14}N_4O_4S_2$ (M+H)$^+$ = 391.0529, found 391.0519 (Figure S10).

**Single Crystal XRD**

The single crystal XRD analysis of **L1** and **L2** was done at Narendrapur Ramkrishna Mission, Kolkata, using a Bruker AXS D8 QUEST ECO diffractometer equipped with monochromatic Mo-target rotating anode X-ray and graphite monochromator α radiation with λ = 0.71073 Å by ω and φ scan technique. The integrated diffraction data, unit cell and data correction were performed by using Bruker SAINT system, SMART and SADABS respectively. The structure was solved by SHELXS-97 through direct method and refined by full matrix least squares based on $F^2$ through SHELXS-2018/3.[1] The hydrogen atoms were added at determined positions as riding atoms and non-H atoms were refined anisotropically. The crystal data and structure refinements of **L1** and **L2** are summarized in Table S1.

**Hirshfeld Surface Analysis**

The Hirshfeld surfaces (HSs) of compounds (**L1**, **L2**, **L2**◻ and **L3**◻) have been carried out based on electron distribution of the molecules and are calculated as the sum of spherical atom electron densities.[2,3] HSs are unique for the investigating molecule and a set of spherical atomic electron densities. The normalized contact distance ($d_{norm}$) is generated based on $d_e$, $di$ and the van der Waals radii of the atom where $d_e$ and $di$ are defined as the distance from the point to the nearest nucleus external and internal to the surface, respectively.[4] The $d_{norm}$ is calculated by the equation

$$d_{norm} = \frac{d_i - r_i^{vdw}}{r_i^{vdw}} + \frac{d_e - r_e^{vdw}}{r_e^{vdw}}$$

The 2D fingerprint plots are generated by using the $d_e$ and $di$ parameters, which elucidate the percentage dominance of particular interaction in developing the supramolecular

architecture.[5,6] The HSs mapped with various properties and 2D fingerprint plots are generated by using the program *CrystalExplorer*.[7]

The contacts that are responsible in the crystal packing in the compounds (**L1**, **L2**, **L2**☐ and **L3**☐) are estimated with respect to their contribution to the crystal structure. We have analysed various HSs for the title compounds that have been mapped over $d_{norm}$ in the range from −0.2500 (red) to 1.1500 (blue) Å, a shape index in the ranges of −1.0 to 1.0 Å and fragment patches (in the ranges of 0.0 to 13.0 Å in **L1**, 0.0 to 17.0 Å in **L2** and 0.0 to 19.0 Å in **L2**☐ & **L3**☐, respectively) (see Figure 5 in the main article)**.** In all compounds, the large circular depression (deep red) on the $d_{norm}$ surfaces, which is evident just above the pyridyl nitrogen atom, designate the N···H/H ···N bonding contacts. Likewise, deep red depressions on the surface of amide oxygen atoms correspond to O···H/H···O contacts. Other light-coloured depressions on the $d_{norm}$ surface are an indicator of weaker contacts. The shape index is the most sensitive to very subtle changes in the surface shape, the red patches on them (above the plane of the molecule) represent concave regions indicating the atoms of the π–π stacked molecule above them, and the blue areas represent convex regions indicating the ring atoms of the molecule inside the surfaces. The nearest neighbour environment of a molecules is identified from the colour patches on fragment patches surfaces depending on their closeness to adjacent molecules. The scattered points of the fingerprint plots[5, 6] evidence all interactions involved within the structures. To quantify each individual contact, we have decomposed the full-fingerprint plots in unique visual mode (Figure S19). The very strong N···H/H···N interactions in all compounds are evidenced by the sharp tips in the region ($de = di \simeq 1.2$Å) contributes 11.6%, 13.7%, 15.7% and 13.8% in **L1**, **L2**, **L2**☐ and **L3**☐, respectively.
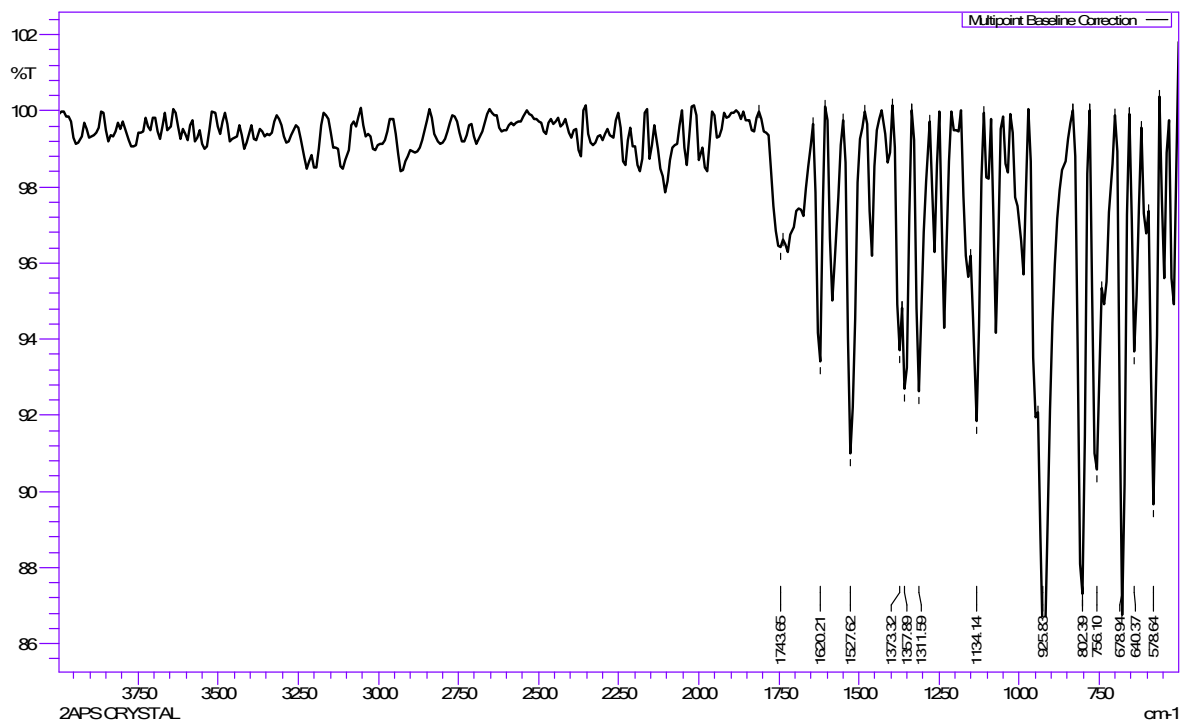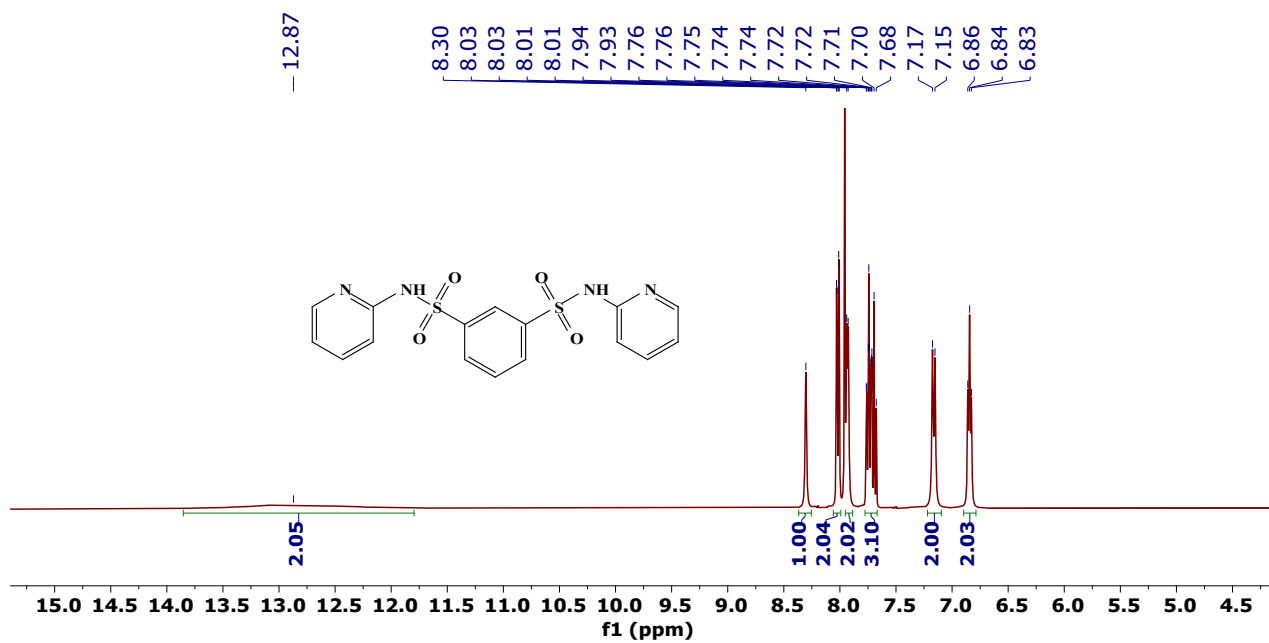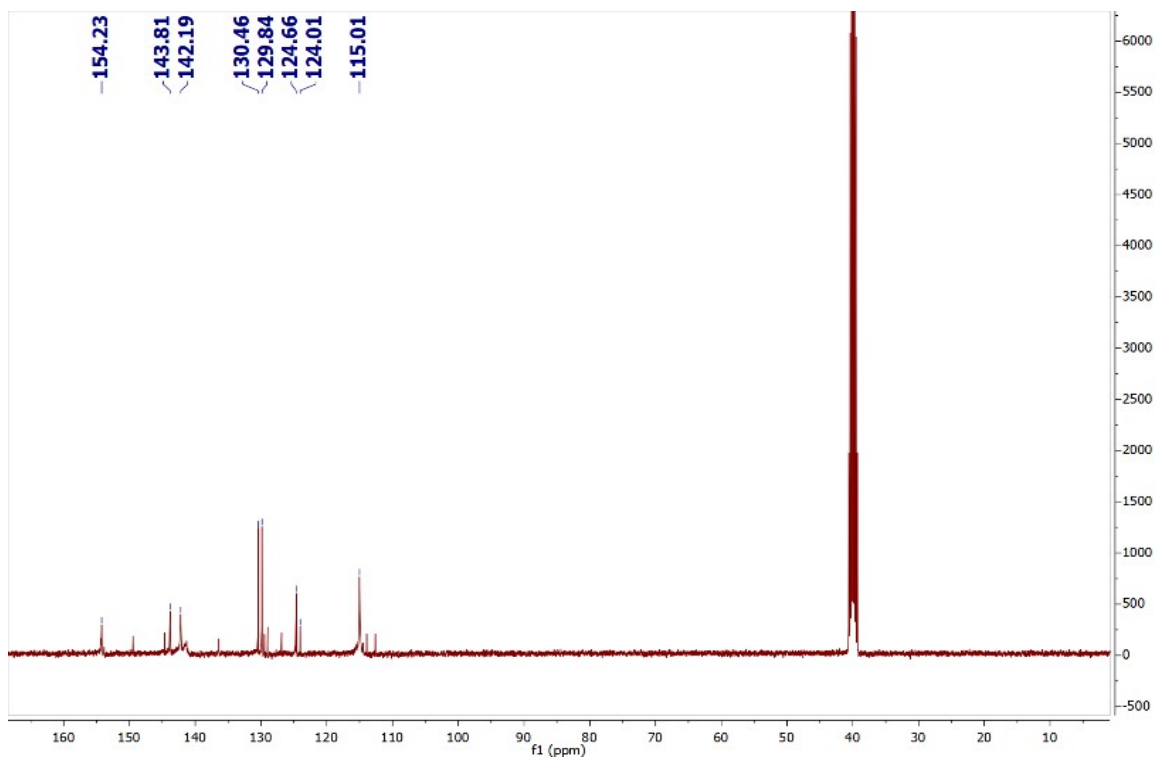
**Figure S1**: IR spectra of **L1**



**Figure S2**: $^1$H-NMR spectra of **L1**

**Figure S3**: $^{13}$C-NMR spectra of **L1**
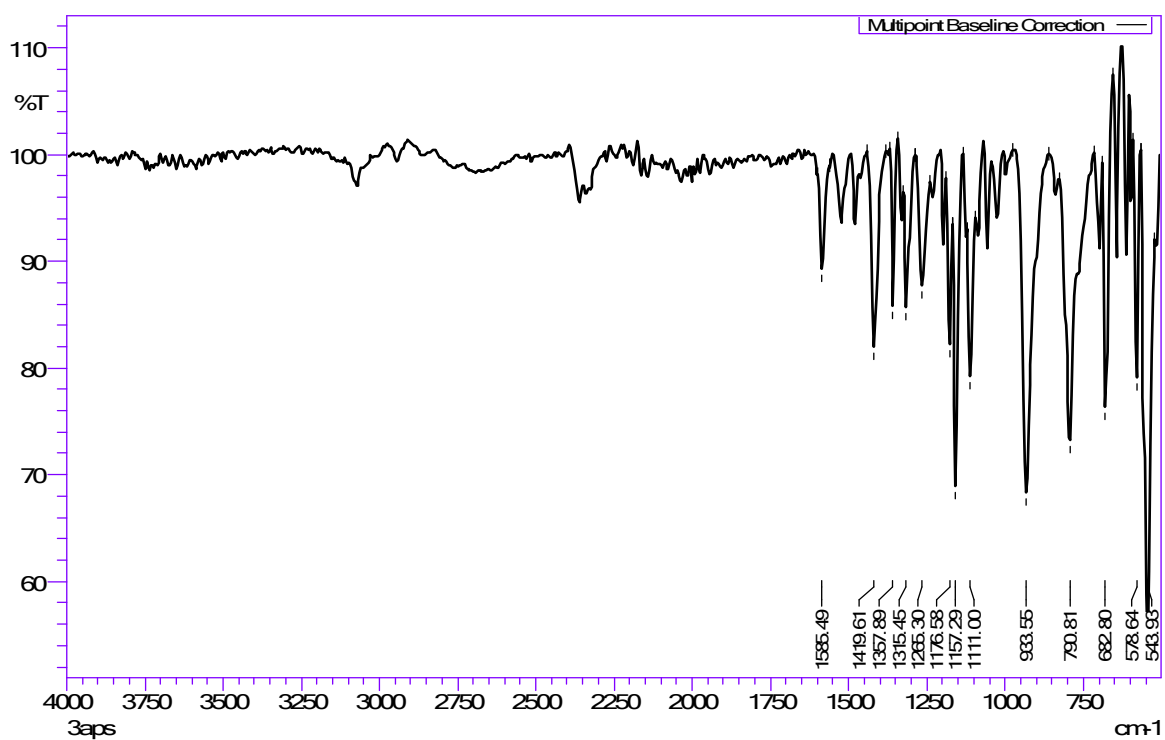


**Figure S4**: IR spectra of **L2**
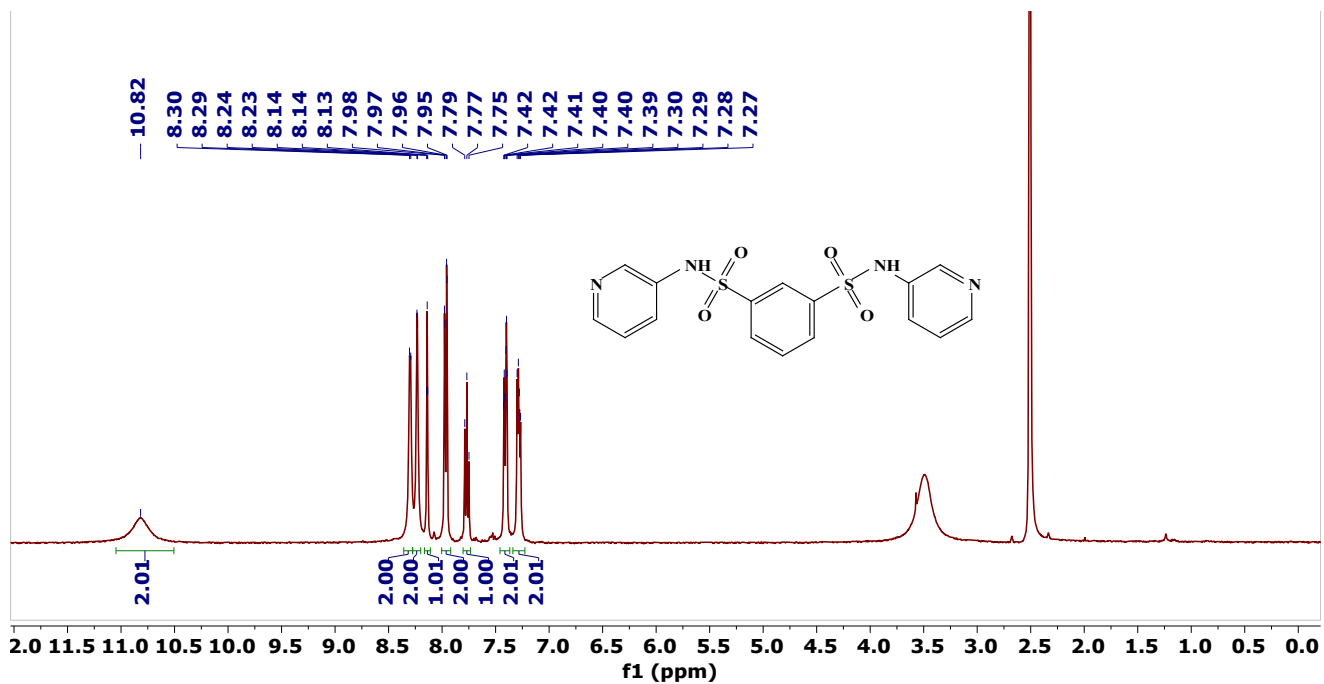
**Figure S5**: $^1$H-NMR spectra of **L2**
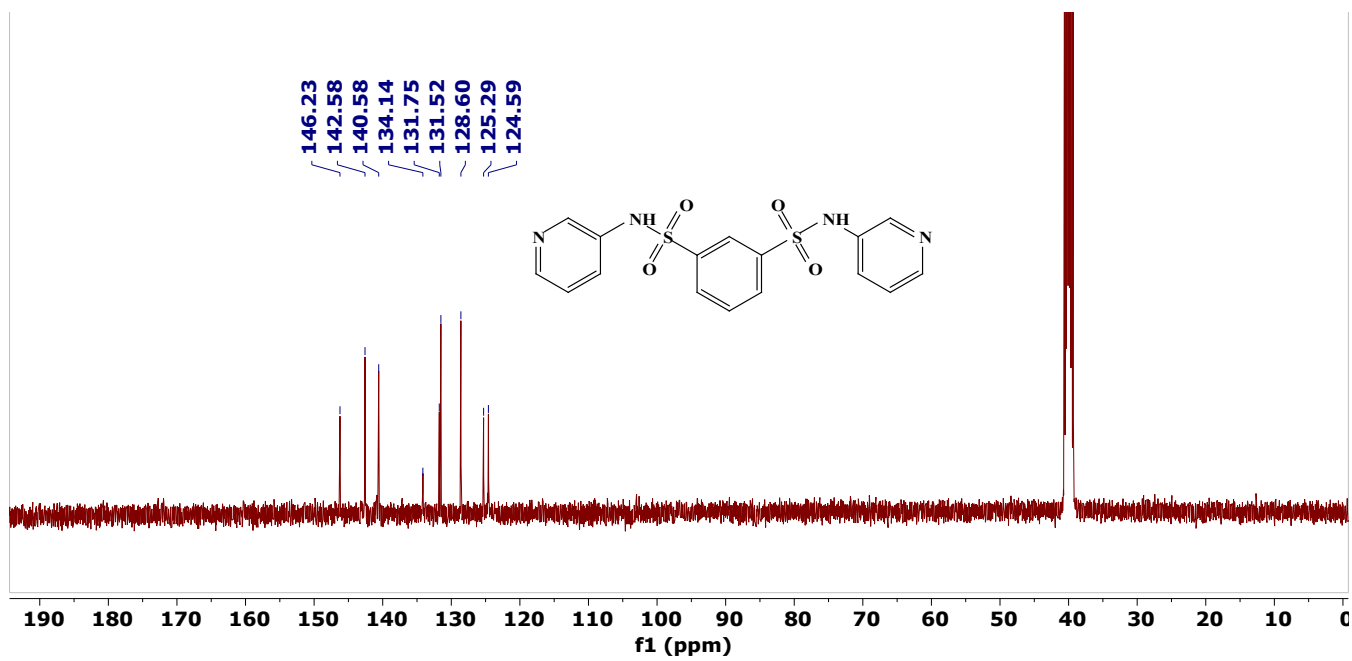


**Figure S6**: $^{13}$C-NMR spectra of **L2**
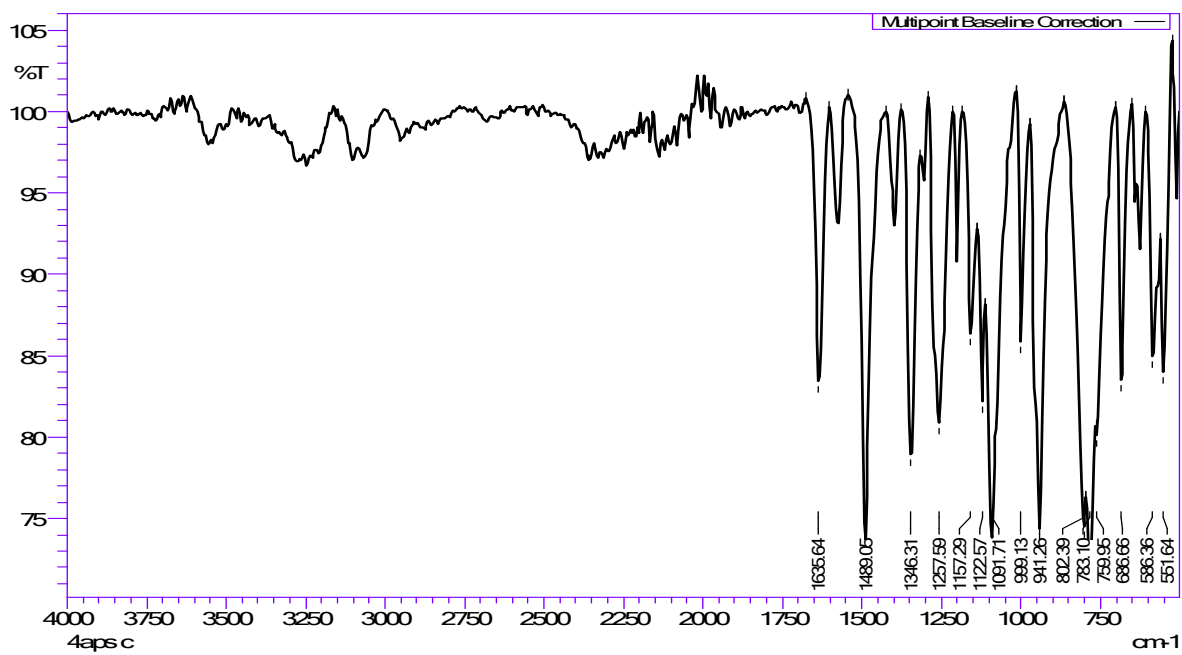
**Figure S7**: IR spectra of **L3**
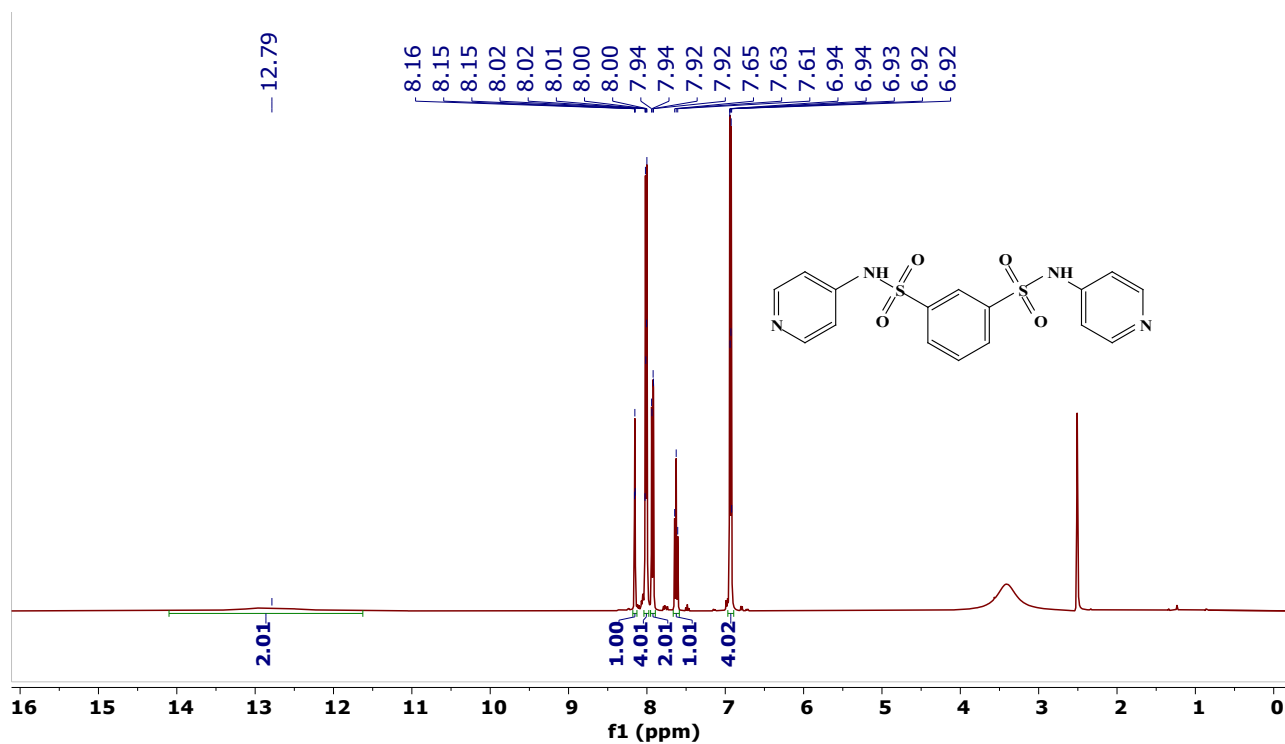


**Figure S8**: $^1$H-NMR spectra of **L3**
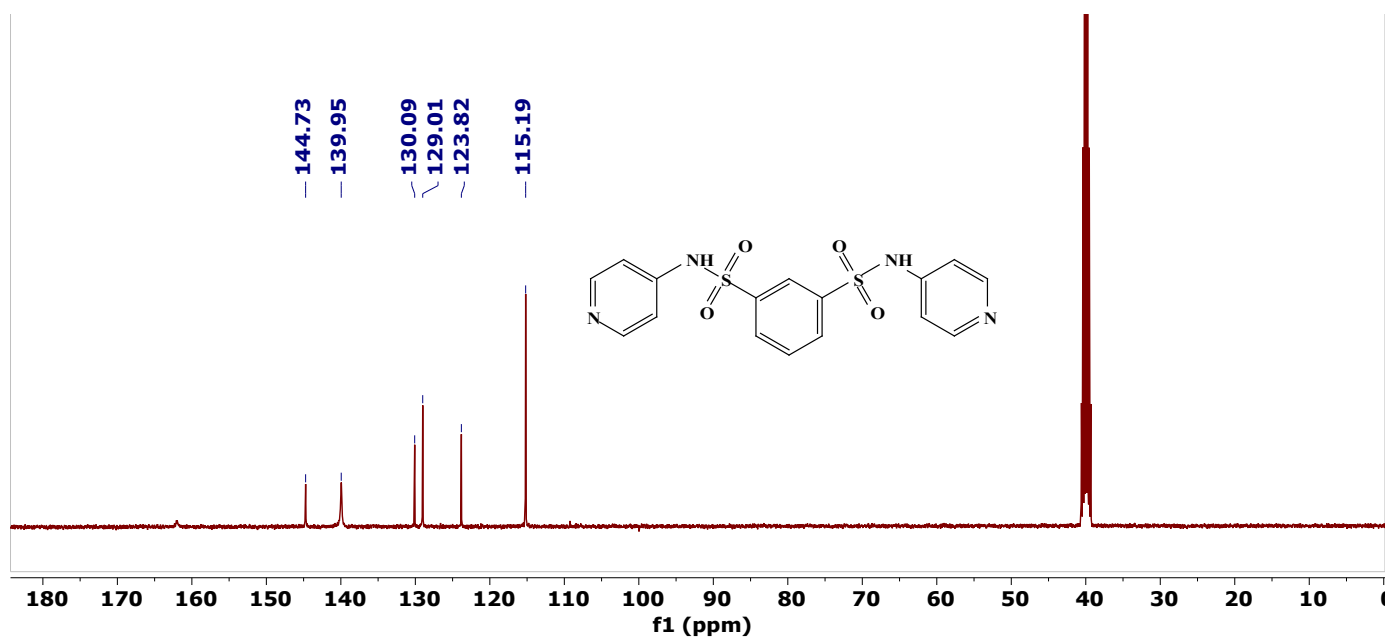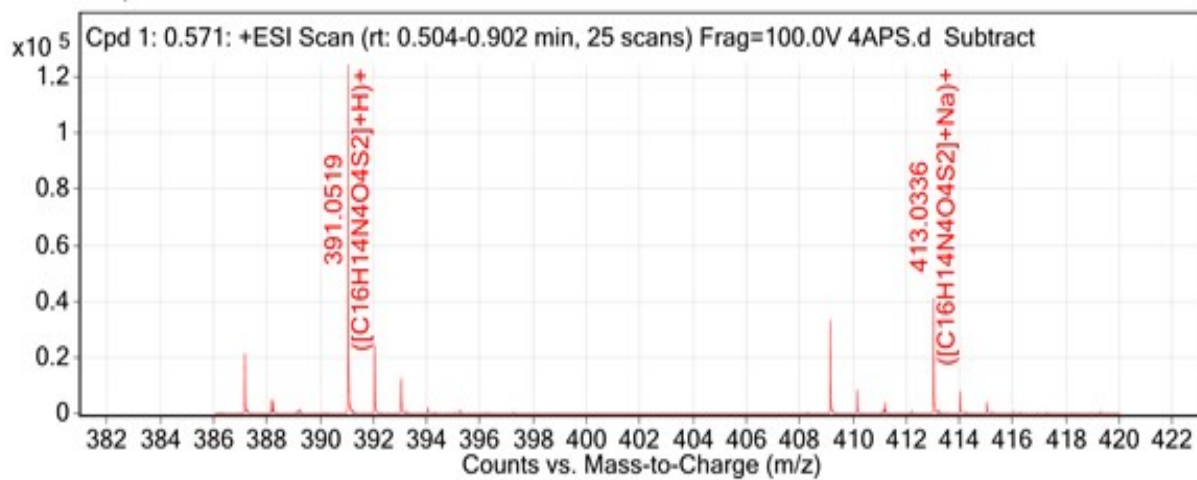
**Figure S9**: $^{13}$C-NMR spectra of **L3**



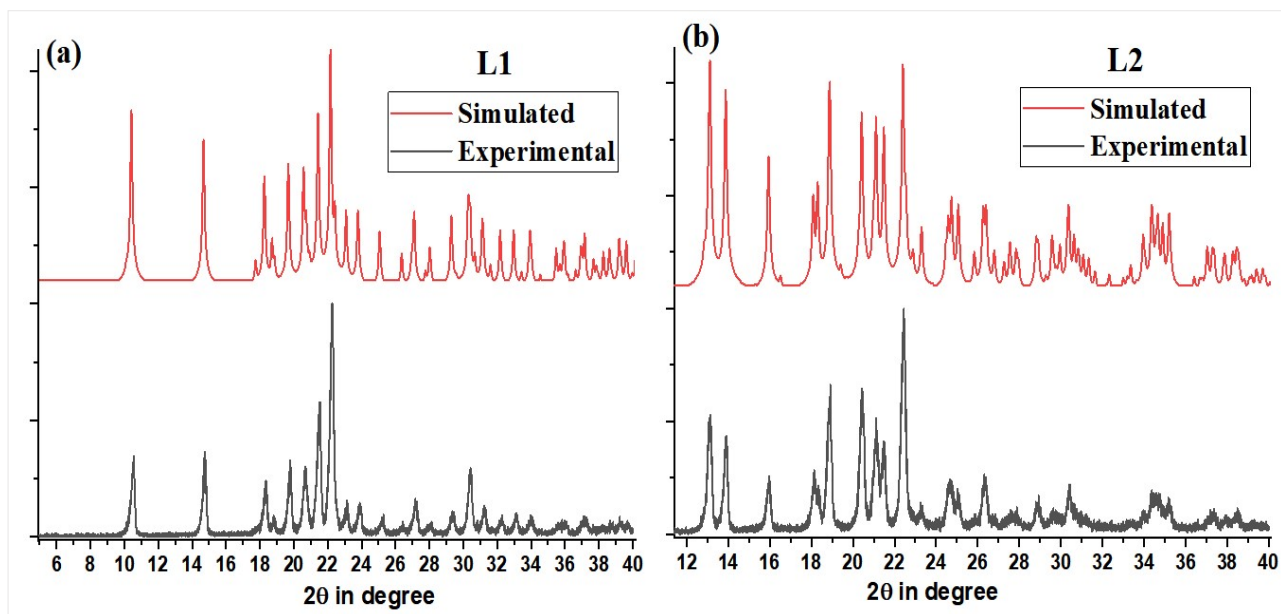**Figure S10**: HRMS of **L3**

**Figure S11**: (a) Experimental and simulated powder XRD of **L1**; (b) Experimental and simulated powder XRD of **L2**
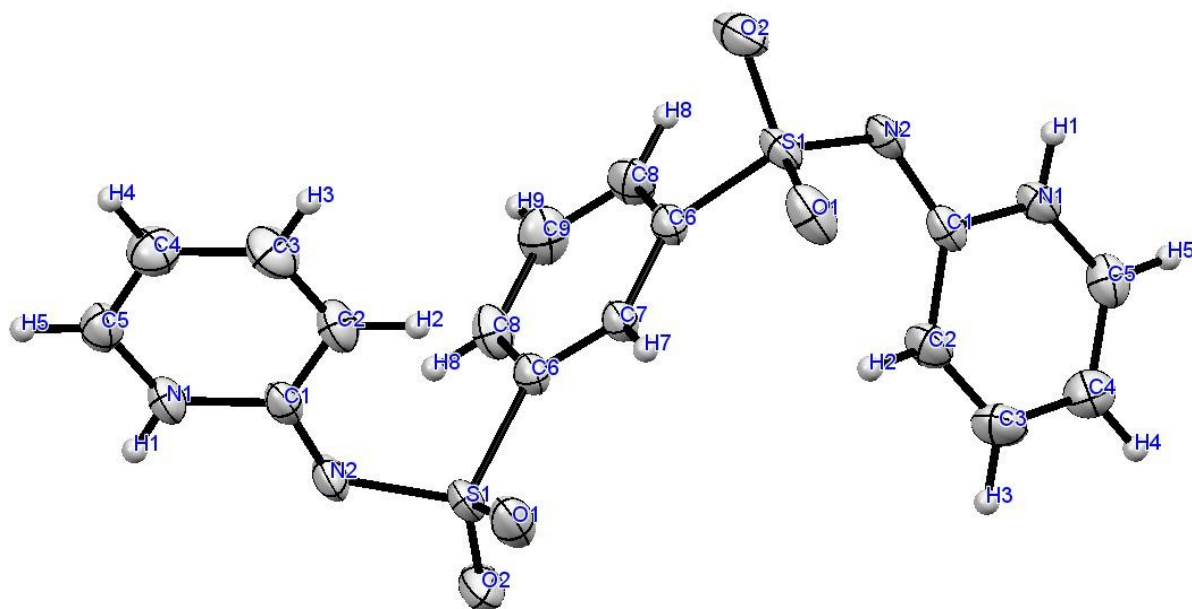


**Figure S12:** ORTEP of **L1** showing thermal ellipsoids at the 50% probability level
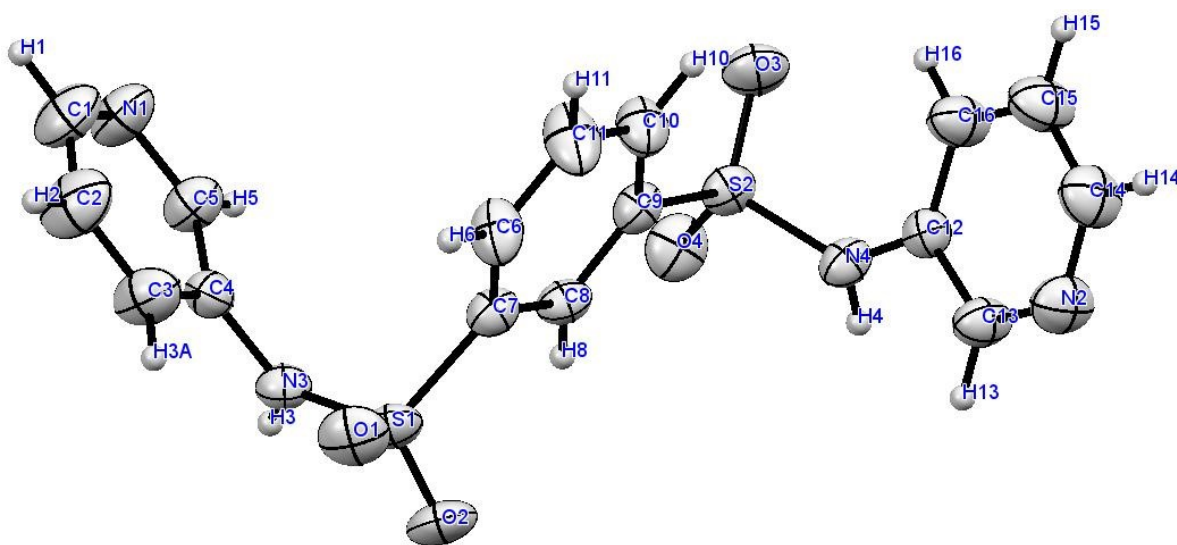
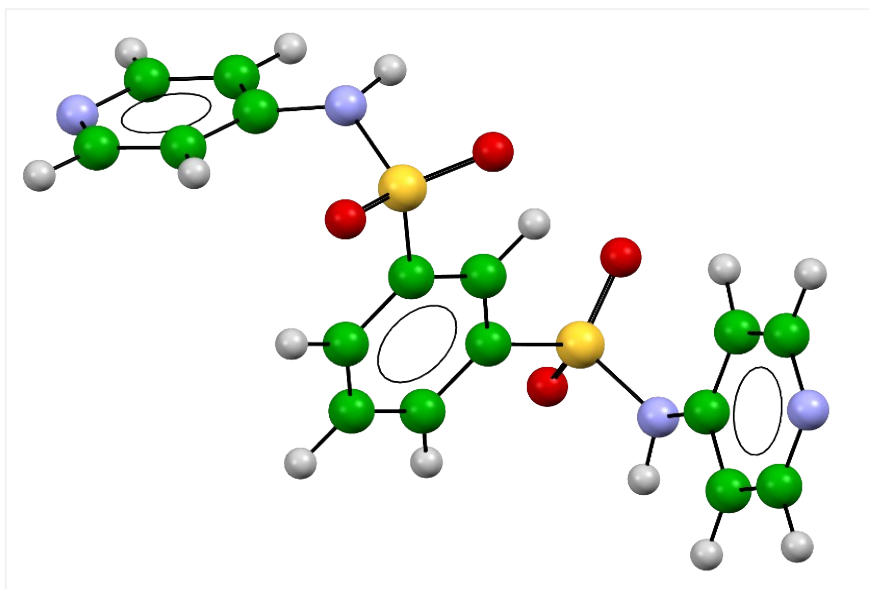**Figure S13:** ORTEP of **L2** showing thermal ellipsoids at the 50% probability level
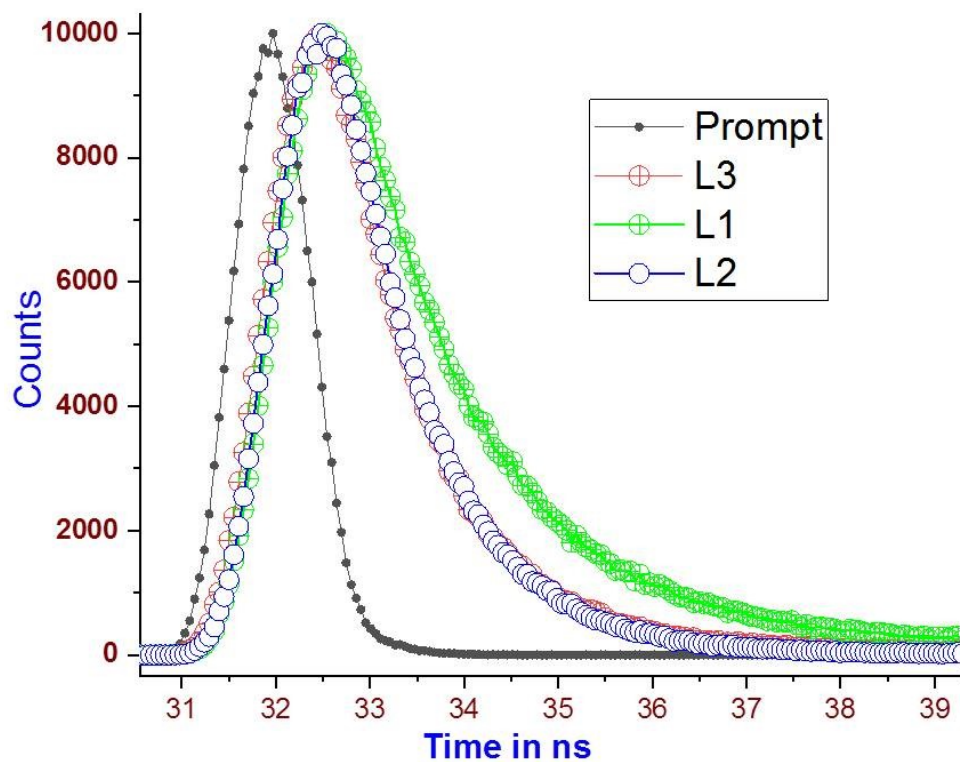


**Figure S14:** Optimized structure of **L3**

**Figure S15:** TCSPC decay profiles of **L1**-**L3** in MeOH with excitation at 340 nm
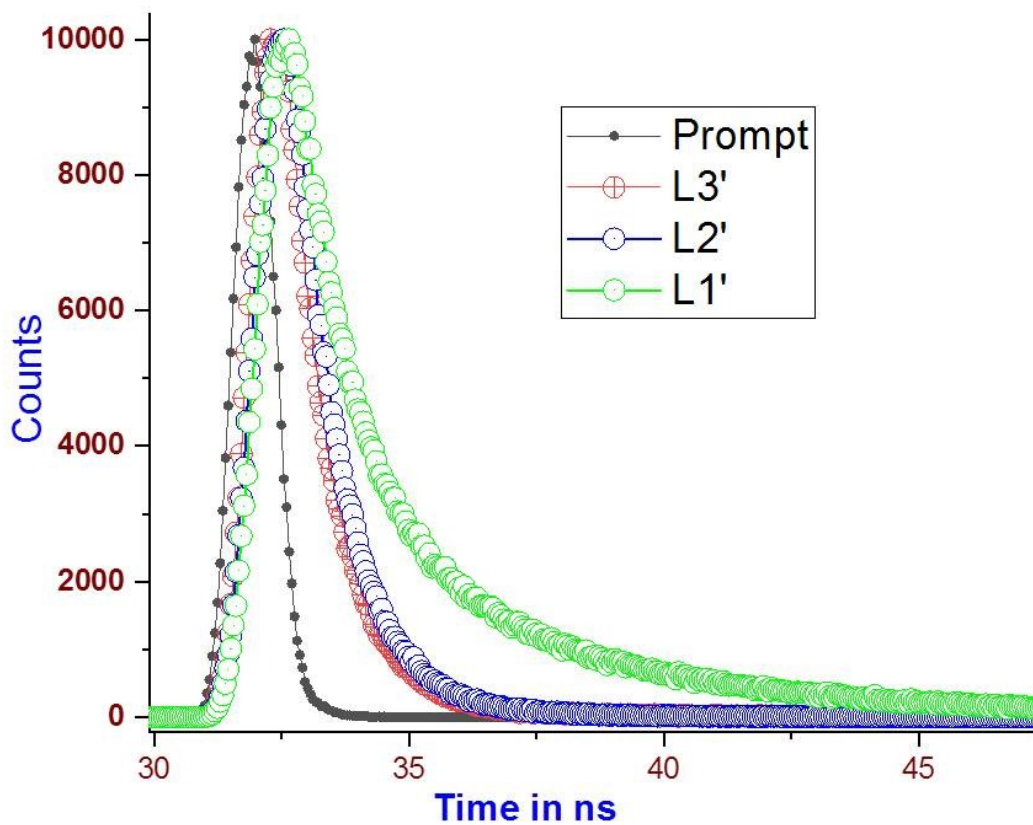


**Figure S16:** TCSPC decay profiles of **L1'**-**L3'** in MeOH with excitation at 340 nm
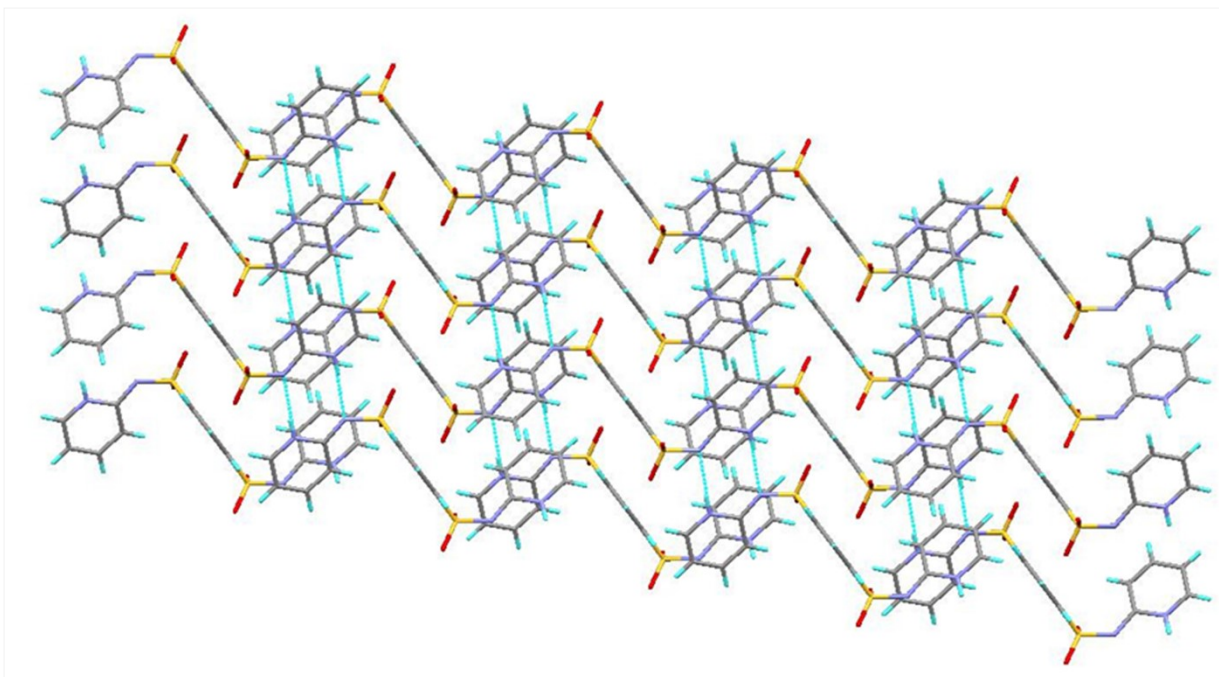
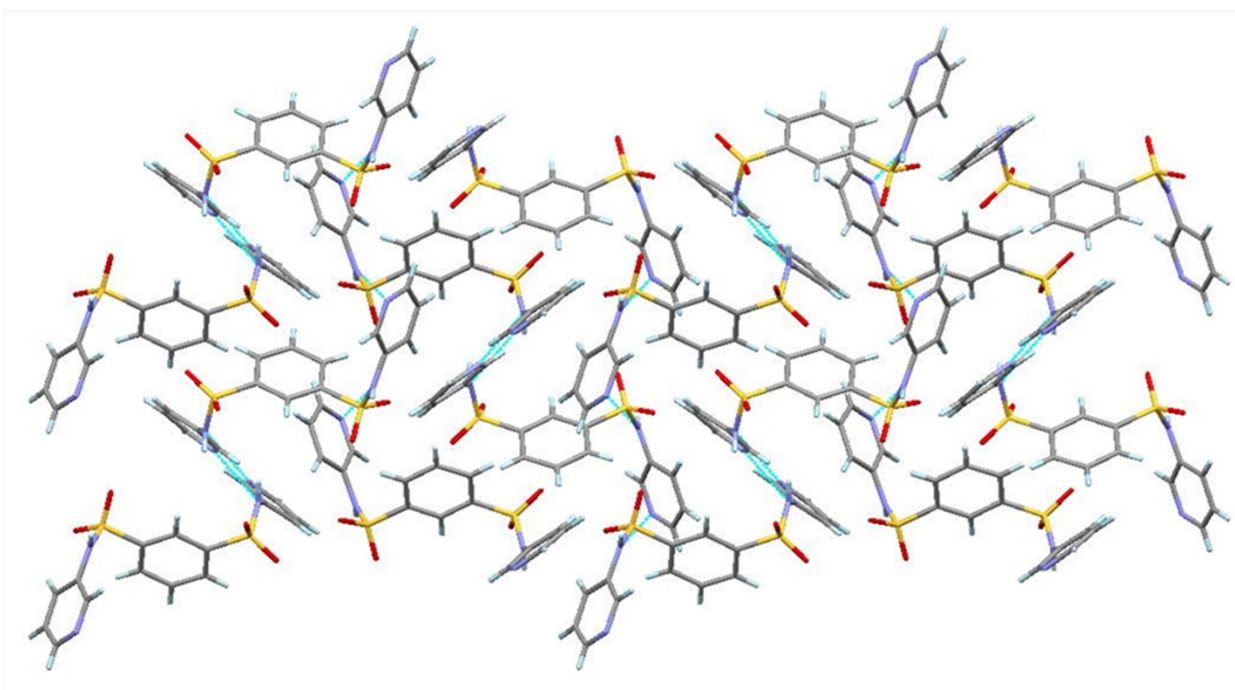**Figure S17**: Assembling of 1D chains of **L1**(View along b- axis)



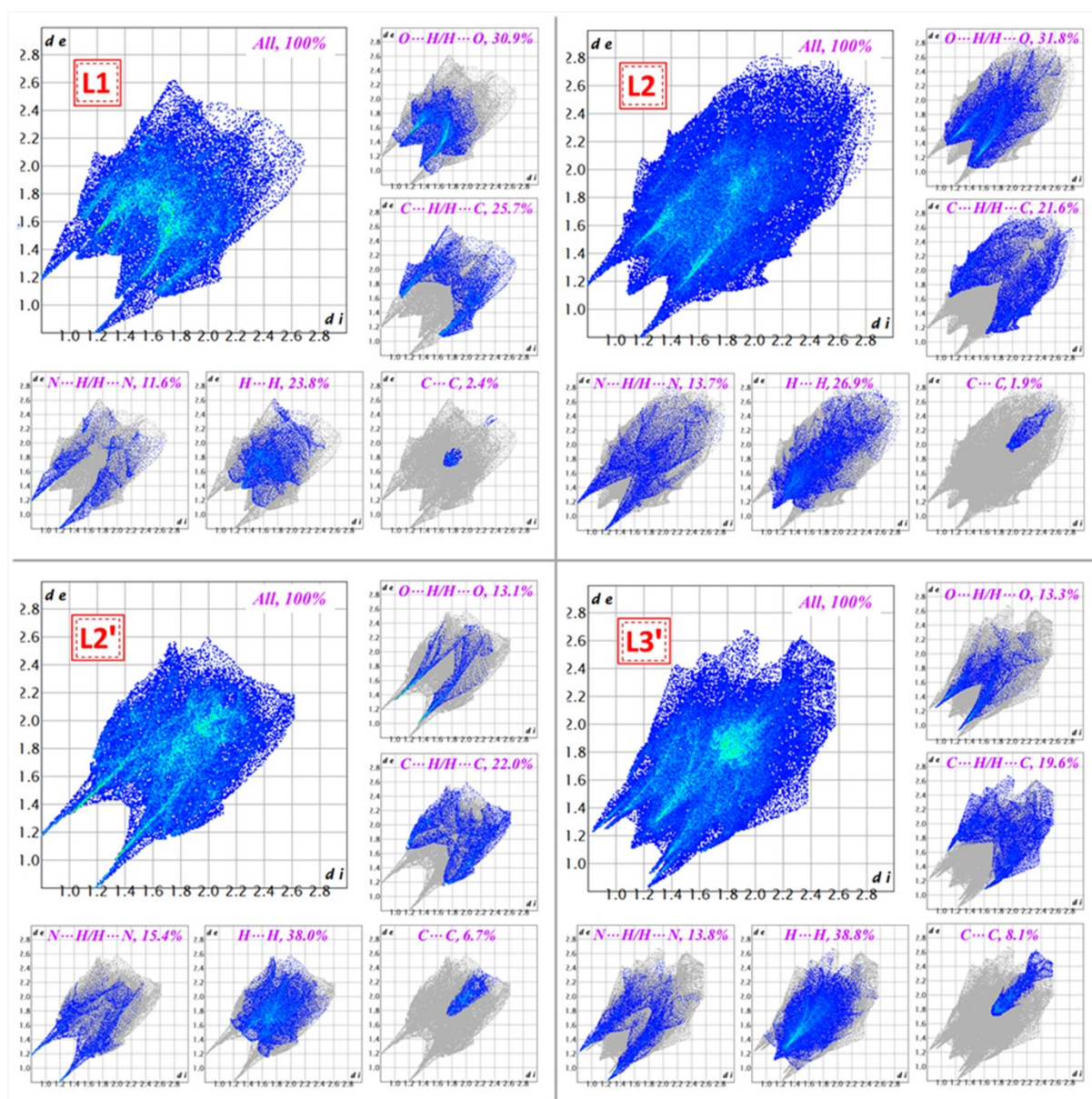**Figure S18:** Assembling of 1D chains of **L2**(View along b- axis)

**Figure S19:** Full and decomposed 2D-fingerprint plots corresponding to various contacts involved within the structure of compound **L1**, **L2**, **L2'** and **L3'**

| | **L1** | **L2** |
|---|---|---|
| | **Table S1**: Crystallographic data of **L1** and **L2** | |
| Chemical formula | $C_{16}H_{14}N_4O_4 S_2$ | $C_{16}H_{14}N_4O_4 S_2$ |
| Formula weight | 390.43 | 390.43 |
| Temperature (K) | 297(2) | 293(2) |
| Wavelength (Å) | 0.71073 | 0.71073 |
| Crystal system | Monoclinic | Orthorhombic |
| Space group | $C2/c$ | $P\,2_12_12_1$ |
| $a$ (Å) | 17.7885(9) | 9.3978(5) |
| $b$ (Å) | 9.7086(4) | 9.6887(5) |
| $c$ (Å) | 9.5753(4) | 19.6049(11) |
| $\alpha$ (°) | 90 | 90 |
| $\beta$ (°) | 100.825(4) | 90 |
| $\gamma$ (°) | 90 | 90 |
| $Z$ | 4 | 4 |
| Volume (Å³) | 1624.24(13) | 1785.07(17) |
| Density (g/cm³) | 1.597 | 1.453 |
| $\mu$ (mm⁻¹) | 0.361 | 0.328 |
| Theta range | 3.083° to 24.729° | 2.345° to 28.250° |
| F(000) | 1760 | 2556 |
| Reflections collected | 5708 | 28332 |
| Independent reflection | 1375 | 4409 |
| Reflections with $I > 2\sigma(I)$ | 1218 | 4209 |
| $R_{int}$ | 0.0315 | 0.0418 |
| Number of parameters | 119 | 235 |
| GO F on $F^2$ | 1.073 | 1.046 |
| Final $R_1{}^a/wR_2{}^b$ ($I > 2\sigma(I)$) | 0.0386 | 0.037 |
| Largest diff. peak and hole (eÅ⁻³) | 0.665 & -0.627 | 0.225 & -0.435 |

[a] $R_1 = \sum||F_o| - |F_c||/\sum|F_o|$. [b] $wR_2 = [\sum w(F_o{}^2 - F_c{}^2)^2/\sum w(F_o{}^2)^2]^{1/2}$, where $w = 1/[\sigma^2(F_o{}^2) + (aP)^2 + bP]$, $P = (F_o{}^2 + 2F_c{}^2)/3$.

**References:**

[1] G. M. Sheldrick, *Acta Crystallogr., Sect. C: Struct. Chem.,* **2015**, 71(1), 3-8.

[2] J. J. McKinnon, A. S. Mitchell and M. A. Spackman, *Chem. – Eur. J.*, 1998, **4**, 2136–2141

[3] M. A. Spackman and D. Jayatilaka, *CrystEngComm*, 2009, **11**, 19–32

[4] F. L. Hirshfeld, *Theor. Chim. Acta*, 1977, **44,** 129–138.

[5] J. J. McKinnon, D. Jayatilaka and M. A. Spackman, *Chem. Commun.*, 2007, **267**, 3814–3816

[6] M. A. Spackman and J. J. McKinnon, *CrystEngComm,* 2002, **4**, 378–392.

[7] P. R. Spackman, M. J. Turner, J. J. McKinnon, S. K. Wolff, D. J. Grimwood, D. Jayatilaka and M. A. Spackman, *J. Appl. Cryst.,* 2021, **54**, 1006–1011.